

Fermi surface dichotomy on systems with fluctuating order

M. Grilli,^{1,2} G. Seibold,³ A. Di Ciolo,^{1,2} and J. Lorenzana^{2,4}

¹*Dipartimento di Fisica, Università di Roma “La Sapienza”, P.le Aldo Moro 5, I-00185 Roma, Italy*

²*SMC-INFN-CNR, Università di Roma “La Sapienza”, P.le Aldo Moro 5, I-00185 Roma, Italy*

³*Institut für Physik, BTU Cottbus, PBox 101344, 03013 Cottbus, Germany*

⁴*ISC-CNR, Via dei Taurini 19, I-00185, Roma, Italy*

(Dated: June 21, 2024)

We investigate the effect of a dynamical collective mode coupled with quasiparticles at specific wavevectors only. This coupling describes the incipient tendency to order and produces shadow spectral features at high energies, while leaving essentially untouched the low energy quasiparticles. This allows to interpret seemingly contradictory experiments on underdoped cuprates, where many converging evidences indicate the presence of charge (stripe or checkerboard) order, which remains instead elusive in the Fermi surface obtained from angle-resolved photoemission experiments.

PACS numbers: 74.72.-h, 74.25.Jb, 71.18.+y, 71.45.-d

I. INTRODUCTION

Strongly correlated systems like the heavy fermions and the superconducting cuprates display excitations over a variety of energy scales. On short timescales (high energies) electrons are excited incoherently over energies ranging from the highest local (Hubbard U) repulsion to the magnetic superexchange interaction. On the other hand, over long timescales, i.e. at low energies around the Fermi level, the excitations can acquire a coherent character typical of the long-lived Fermi-liquid quasiparticles (QPs). These energy scales appear very clearly both in theoretical¹ and experimental² studies of the one particle spectral function of strongly correlated systems. It is usually assumed that the incoherent part has no momentum structure, an assumption which is emphasized by infinite dimensional studies where the self-energy is momentum independent and spacial information on quasi long range correlations close to a phase transition are lost.¹

In this paper we discuss how this picture is modified in physical spatial dimensions. We want to address how the spectral function looks like when the system is close to an ordered phase. This issue is particularly important in the context of cuprates where it has been proposed that some kind of stripe-like order fluctuates in the metallic phase.^{3,4,5}

The scenario that we propose is based on the following qualitative argument: In physical dimensions a system may have long (but finite) ranged order parameter spacial correlations which are also long lived close to a quantum critical point. This defines a fluctuating frequency ω_0 above which the systems appears to be ordered. We argue that for energies larger than ω_0 with respect to the Fermi level the spectral should resemble the spectra function of an ordered system. This spectral weight resides in what is usually called the incoherent part, which we argue, can have some important momentum structure. On the other hand at lower energies electrons average over the order parameter fluctuations and “sense” a disordered system. In this limit we expect Fermi liquid quasiparticles with all their well known characteristics

like a Luttinger Fermi surface (FS).

To understand the momentum structure of the spectral function at energies higher than ω_0 is important because if the incoherent part carries a memory of the close by ordered phase it should be possible to analyze it to obtain information on what is the underlying fluctuating order. Usually ordered systems are well described by mean-field thus one can obtain a first guess of how the incoherent part of the spectral function in the disordered phase should look like by performing a mean-field computation assuming long-range order. Comparison with experimental data in the absence of long range order can be useful to identify the fluctuating order parameter.

To fix ideas consider as an example a moderately large U Hubbard system in a half-filled bipartite lattice in two dimensions at $T = 0$. In this case an antiferromagnetic state is expected to be a competitive low-energy state. When the system is in the ordered phase the spectral function will be reasonably well described by a mean-field computation and will show two Hubbard bands separated in energy by mU with m the staggered magnetization. The bands will show some dispersion governed by the scattering of the electrons with the mean-field potential. Suppose that due to some frustrating effect long range magnetic order is lost while keeping well formed magnetic moments. We expect that beyond mean field if U is not too large (so that the disordered phase is metallic) a quasiparticle will appear at the center of the Hubbard bands with small spectral weight resembling the dynamical mean field theory (DMFT) picture.¹ At high energies, however, electrons will sense a mean-field like staggered potential for distances of the order of the correlation length ξ , which can be quite long, and therefore the system will keep substantial memory of the mean-field like bands with their dispersion. Roughly we expect that the spectral function will look like the superposition of a Fermi liquid like spectral function, with a small weight z close to the Fermi level, plus a blurred mean-field-like spectral function in the presence of long-range order with a large weight $1 - z$. This is at first sight similar to the DMFT picture but it differs in that in

DMFT there are no magnetic correlations surviving in the disordered phase and the incoherent part becomes momentum independent whereas at finite dimension we will show that the incoherent part carries important information encoded in the momentum dependence.

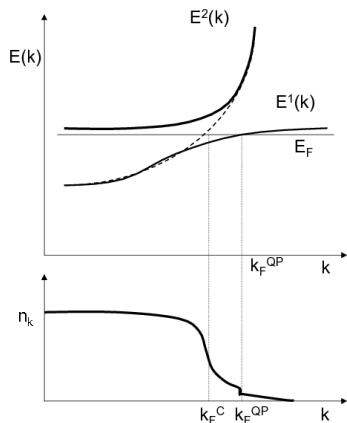


FIG. 1: Schematic view of heavy-fermion system with a Kondo-like resonance arising at the Fermi energy E_F from the mixing of a deep narrow f level (not shown) and the conduction band (dashed line). Two QP bands arise $E^{1,2}(k)$. The corresponding momentum distribution function $n_{\mathbf{k}}$ is shown below with a true Fermi momentum k_F^{QP} and a “fictitious” Fermi surface at k_F^c .

Another example can clarify the concept of an incoherent part with a strong momentum dependence which carries physical information on the short range physics. Lets consider the more standard issue of large and small FSs in heavy fermions represented in Fig. 1. In heavy fermions strongly correlated electrons in a narrow half-filled f level hybridize with electrons in a conduction band and give rise to a Kondo resonance at the Fermi level formed by coherent QP states. The width (and weight) of this QP band is usually quite small and sets the scale of the coherence energy in these systems. Now consider the momentum distribution function defined by:

$$n_{\mathbf{k}} \equiv \int d\omega A(\mathbf{k}, \omega) f(\omega), \quad (1)$$

where $f(\omega)$ is the Fermi function and the spectral density

$$A(\mathbf{k}, \omega) \equiv \frac{1}{\pi} \text{Im} G(\mathbf{k}, \omega) = \frac{1}{\pi} \frac{\Sigma''(\mathbf{k}, \omega)}{(\omega - \Sigma'(\mathbf{k}, \omega))^2 + \Sigma''^2(\mathbf{k}, \omega)} \quad (2)$$

is proportional to the imaginary part of the electron Green function with real (imaginary) part of the self-energy Σ' (Σ''). It is crucial to recognize that $n_{\mathbf{k}}$ involves all the excitation energies and its features might be dominated by the incoherent part of the spectrum if the QPs

have a minor weight. Indeed strictly speaking the true FS at zero temperature is given by the small jump in the Fermi distribution function determining the Fermi momenta of the QPs at \mathbf{k}_F^{QP} . This FS is large and satisfies the Luttinger theorem with a number of carriers including the electrons in the f level. This FS would naturally be determined by following the QP dispersion. On the other hand the shape of $n_{\mathbf{k}}$ is substantially determined by the (incoherent) part of the spectral function, which has strong weight at energies corresponding to both the f level and the conduction band. This latter gives rise to a rather sharp decrease of $n_{\mathbf{k}}$ at a “fictitious” Fermi momentum \mathbf{k}^c , corresponding to the FS that the electrons in the conduction band would have in the absence of mixing with the f -level. If the hybridization between the f level and the conduction band is turned off so that the quasiparticle weight z is driven to zero one reaches a situation in which the decrease at \mathbf{k}^c becomes a discontinuity and the small jump at \mathbf{k}_F^{QP} disappears. This shows that a computation in which the fluctuating order is artificially frozen can give some hints on the distribution of the incoherent spectral weight in the less trivial case with fluctuations. Mutatis mutandis it is clear that the sharp decrease of spectral weight at \mathbf{k}^c for finite hybridization has strong physical content for an observer who ignores the underlying model.

The above ideas but with a more complicated order parameter may explain perplexing data on cuprates. Several years ago underdoped $\text{La}_{2-x}\text{Sr}_x\text{CuO}_4$ (LSCO compounds) were examined and a dichotomy was found in the Fermi surface (FS) determined by two different treatments of the data. On the one hand the momentum dependence of the low-energy part of the energy distribution curves was followed thereby reconstructing the low-energy QP dispersion. In this way a large FS was found corresponding to the Fermi liquid LDA band-structure and fulfilling the Luttinger requirement that the volume of the FS encircled the whole number of fermionic carriers $n = 1 - x$. On the other hand the FS was determined from the momentum distribution $n_{\mathbf{k}}$ obtained integrating the spectral function over a broad energy window (~ 300 meV). Then the locus of momentum-space points where $n_{\mathbf{k}}$ displays a sharp decrease marked a FS formed by two nearly parallel (weakly modulated) lines along the k_x direction and crossing two similar lines along the k_y direction. This crossed FS would naturally arise in a system with one-dimensional stripes along the x and y directions.

As a matter of fact the stripe Fermi surface has been observed both in system which show a striped ground state and in systems where long-range stripe order has not been detected.^{6,7} As in the heavy Fermion case for relatively small z we expect that $n_{\mathbf{k}}$ is dominated by the incoherent spectral weight. According to our scenario $n_{\mathbf{k}}$ should resemble the Fermi surface of stripes in mean-field regardless of whether stripe order is static or fluctuating at low frequencies. Indeed LDA computations in the presence of stripes with magnetic and charge long-range

order reproduce this Fermi surface.⁸

The experimental stripe-like Fermi surface is not flat as could be expected for a perfect one dimensional band structure but shows some wavy features, which depend on the details of residual hopping processes perpendicular to the stripes. Remarkably the wavy features are well reproduced by the LDA computation both with regard to amplitude and periodicity giving credibility to the idea that the static LDA computation provides a snapshot of the fluctuating order in the disordered phase.

The main point is that the formation of quasiparticles due to some coherence effect is a small perturbation for the overall distribution of spectral weight. Thus a careful study of $n_{\mathbf{k}}$ can give precious information on the proximity to some order phase. By the same token the presence of quasiparticles and a Fermi-liquid-like Fermi surface are not incompatible with two-particle responses (neutrons, optical) which show strong features of ordering (like stripes) at frequencies above ω_0 . This explains why computations of fluctuations on top of stripe phases with long range order^{9,10} explain well optical conductivity and neutron scattering data of systems without long-range order.

In the following section we present a toy model of the Kampf-Schrieffer-type¹¹ where the dichotomy between a Fermi-liquid-like Fermi surface and a momentum dependent incoherent part, reflecting the fluctuating order, can be illustrated. Although we study self-energy corrections self-consistently the lack of vertex corrections make our computations reliable only in weak coupling where quasiparticle weights are close to one. Within this limitation one can show that the described scenario holds.

In Sec. II we present the model, while in Sec. III we present some numerical results. A discussion of the results and our conclusions are reported in Sec. IV.

II. THE MODEL

In order to substantiate the above ideas we consider a system of electrons coupled to a dynamical order parameter which can describe charge ordering (CO) fluctuations or spin ordering (SO) fluctuations or both. To fix ideas we consider CO fluctuations described by an effective action

$$S = -g^2 \sum_{\mathbf{q}} \int_0^\beta d\tau_1 \int_0^\beta d\tau_2 \chi_{\mathbf{q}}(\tau_1 - \tau_2) \rho_{\mathbf{q}}(\tau_1) \rho_{-\mathbf{q}}(\tau_2). \quad (3)$$

In order to simplify the calculations we consider a Kampf-Schrieffer-type model susceptibility¹¹ which is factorized into an ω - and \mathbf{q} -dependent part, i.e.

$$\chi_{\mathbf{q}}(i\omega) = W(i\omega)J(\mathbf{q}) \quad (4)$$

The (real-frequency)-dependent part is $W(\omega) = \int d\nu F_{\omega_0, \Gamma}(\nu) 2\nu / (\omega^2 - \nu^2)$, with $F_{\omega_0, \Gamma}$ being a normalized lorentzian distribution function centered around ω_0

with half-width Γ , $F_{\omega_0, \Gamma}(\omega) \sim \Gamma / [(\omega - \omega_0)^2 + \Gamma^2]$. The momentum-dependent part in D dimensions reads

$$J_D(\mathbf{q}) = \mathcal{N} \sum_{\eta=1}^D \sum_{\pm Q_\eta} \frac{\gamma}{\gamma^2 + D - \cos(q_\eta - Q_\eta)}. \quad (5)$$

\mathcal{N} is a suitable normalization factor introduced to keep the total scattering strength constant while varying $\gamma \propto \xi^{-1}$ (with ξ the CO/SO correlation length). To simplify the treatment and to make the effect of fluctuations as clear as possible, we will mostly consider the case of spatially coherent fluctuations. Although formally the correlation length ξ diverges the ordering is not static and we will show that this is enough for the spectral function to converge to the Fermi-liquid Fermi surface at zero frequency.

The infinite correlation length case is described in D dimensions by,

$$J_D(\mathbf{q}) = \frac{1}{4} \sum_{\eta=1}^D \delta(q_\eta - Q_\eta) + \delta(q_\eta + Q_\eta). \quad (6)$$

In previous works the spatially-smeared version of $J_D(\mathbf{q})$, Eq. (5), was considered to describe the kink in the electron dispersions¹² and the (still experimentally controversial^{13,14}) isotopic dependence of these dispersions.¹⁵ The susceptibility χ contains the charge-charge correlations in the case of charge fluctuations and spin-spin correlations in the case of magnetic fluctuations.

If only the dynamical part $W(\omega)$ were present in $\chi_{\mathbf{q}}(i\omega)$, one would have a bosonic spectrum $B(\omega) = \tanh(\omega/(kT))F_{\omega_0, \Gamma}(\omega)$ which is a “smeared” version of the Holstein phonon considered in Ref. 16. The crucial feature of the susceptibility (4) is the substantial momentum dependence, which describes the (local) order formation and reflects the proximity to an instability with broken translational symmetry.

The static limit $F_{\omega_0, \Gamma}(\nu) = \delta(\nu - \omega_0)$ together with an infinite charge-charge correlation length ($\gamma \rightarrow 0$) as the one considered in Eq. (6) reproduces mean-field results for a long-range phase.^{11,17} The static limit of (4) has been the object of an intense activity based on the idea, pioneered in Ref. 18, that different types of slow order-parameter (OP) fluctuations (SO¹¹ or CO¹⁷) can be treated as classical fluctuations with time-independent correlations. The equivalence of such static degrees of freedoms with quenched impurities has more recently been formalized and cast in field-theoretical language.¹⁹ Although they allow for (nearly) exact solutions, the main drawback of these static approaches is that they do not allow for the aimed separation of energy (i.e. time) scales since to justify the static character of the OP fluctuations, they assume that their relaxation time τ_{OP} is much longer than the inelastic scattering rate of the electrons τ_e , $\tau_{OP} \gg \tau_e$.¹⁹ Here we consider instead

$$F_{\omega_0, \Gamma}(\nu) = \delta(\nu - \omega_0) \quad (7)$$

representing a *dynamical* fluctuation oscillating at a frequency ω_0 and therefore averaging out on timescales $\tau_{OP} \sim 1/\omega_0$.

In the present limit the problem has also a simple Hamiltonian formulation which we introduce for later use:

$$H = \sum_{\mathbf{k}\sigma} \xi_{\mathbf{k}} c_{\mathbf{k}\sigma}^\dagger c_{\mathbf{k}\sigma} + \omega_0 (b_{\mathbf{Q}}^\dagger b_{\mathbf{Q}} + b_{-\mathbf{Q}}^\dagger b_{-\mathbf{Q}}) \quad (8)$$

$$+ g \sum_{\mathbf{k}\sigma} \left[c_{\mathbf{k}-\mathbf{Q}\sigma}^\dagger c_{\mathbf{k}\sigma} (b_{\mathbf{Q}}^\dagger + b_{-\mathbf{Q}}) + c_{\mathbf{k}+\mathbf{Q}\sigma}^\dagger c_{\mathbf{k}\sigma} (b_{-\mathbf{Q}}^\dagger + b_{\mathbf{Q}}) \right]$$

where $c_{\mathbf{k}\sigma}^\dagger$ creates a free Fermion and $b_{\pm\mathbf{Q}}^\dagger$ creates a bosonic collective mode excitation and $\xi_{\mathbf{k}} \equiv \varepsilon_{\mathbf{k}} - \mu$.

QPs at energies much larger than ω_0 see an essentially static fluctuation and modify their dispersion as in the mean-field calculation mentioned above. For them the fluctuations are static and, if the momentum dependent part $J(\mathbf{q})$ is strongly peaked around the ordering wavevector \mathbf{Q} , they are scattered like in the presence of a long-range symmetry breaking. Their dispersions are modified accordingly. On the other hand, for QPs at energies in a shell of width ω_0 around the Fermi level the order parameter fluctuations are far from being static and have not enough energy to excite them. For these QPs the system is still in a uniform Fermi-liquid metallic state. Therefore, if their dispersion is followed near the chemical potential μ , a large FS fully preserving the Luttinger volume is found. In the following we explicitly calculate the band dispersions and the FS to show this physical mechanism at work and the resulting dichotomy of the FS.

Neglecting vertex corrections we iteratively solve at zero temperature the following coupled set of equations for the self-energy and the Green's function (GF)

$$\Sigma(\mathbf{k}, i\omega) = -\frac{g^2}{\beta} \sum_{\mathbf{q}, ip} \chi_{\mathbf{q}}(ip) G(\mathbf{k} - \mathbf{q}, i\omega - ip) \quad (9)$$

$$G(\mathbf{k}, i\omega) = \frac{1}{i\omega - \xi_{\mathbf{k}} - \Sigma(\mathbf{k}, i\omega)}. \quad (10)$$

To the best of our knowledge our self-consistent treatment goes beyond previous solutions that remained at the perturbative level. The latter can be obtained at lowest order by replacing the GF in Eq. (9) by the non-interacting G^0 . For our specific model of the susceptibility the self-energy becomes:

$$\Sigma^{(1)}(\mathbf{k}, i\omega) = g^2 \left\{ \frac{f(\xi_{\mathbf{k}+\mathbf{Q}})}{i\omega + \omega_0 - \xi_{\mathbf{k}+\mathbf{Q}}} + \frac{1 - f(\xi_{\mathbf{k}+\mathbf{Q}})}{i\omega - \omega_0 - \xi_{\mathbf{k}+\mathbf{Q}}} \right\} \quad (11)$$

where the superscript (1) denotes the order of the iteration and $f(\xi_{\mathbf{k}+\mathbf{Q}}) = \Theta(-\xi_{\mathbf{k}+\mathbf{Q}})$ is the occupation number. Inserting this self-energy into Eq. (10) leads to a GF $G^{(1)}(\mathbf{k}, i\omega)$ which displays now two poles and which can be used to compute $\Sigma^{(2)}(\mathbf{k} + \mathbf{Q}, i\omega)$ (and thus $G^{(2)}(\mathbf{k} + \mathbf{Q}, i\omega)$) and so on. The detailed procedure is described in the Appendix.

For the sake of simplicity, we first implement our numerical analysis in one dimension and then we describe the case of two dimensions, which is more relevant for layered materials.

III. NUMERICAL RESULTS OF FLUCTUATING ORDER

A. Numerical analysis in one dimension

Coherent order parameter fluctuations

We first present the results for a one-dimensional model with a commensurate ordering wavevector $Q = \pi$ corresponding to CO/SO with a doubling of the unit cell. In particular we consider a band of QPs $\varepsilon_{\mathbf{k}} = -\cos(\mathbf{k})$ (we choose a unit hopping parameter $t = 1$ and a unitary lattice spacing) coupled via a CO/SO mode given by Eqs. (4) and (6). Fig. 2 reports the simplest case in which only two poles are considered in the GF given by $G^{(1)}$ for a generic filling ($n = 0.67$: here and in the following densities are defined as total number of particles per site) and for a *static* fluctuation (i.e. $\omega_0 = 0$). This is the

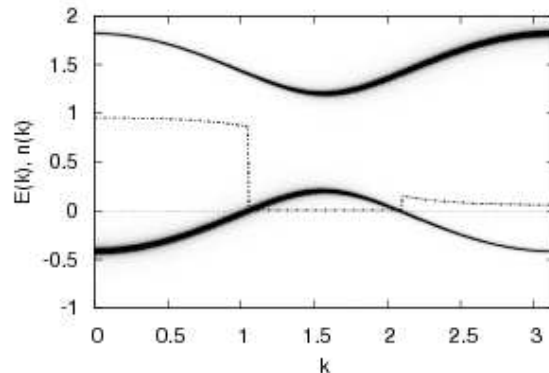


FIG. 2: Two-pole band structure in one dimension for $g = 0.5t$, $\omega_0 = 0$ and particle density $n = 0.67$. The width of the curve is proportional to the weight of the state. The dashed curve is the momentum distribution curve and energies are measured with respect to E_F .

standard mean-field solution, with a doubling of the unit cell and a folding of the bands resulting in a double FS. In the absence of interaction the Fermi momentum would be given by $k_F = n\pi/2 = 1.05$. The dispersion relation instead displays two Fermi points and a very different Fermi surface volume “violating” Luttinger theorem.

The situation is very different for a *dynamical* fluctuation. In Fig. 3 we report the spectral function with $\omega_0 = 0.3$ and moderately weak coupling $g^2/\omega_0 = 0.5$. Also in this case shadow bands appear so that the electronic structure has bands close to the location of the

bands in the broken symmetry state. The shadow bands, however, do not reach the Fermi level and one has only one FS point at $k = k_F$. Therefore the Luttinger theorem is satisfied since the divergent pole in $G(k_F^2, \omega = 0)$ from the static solution now turns into a step so that $G(k, \omega = 0) < 0$ for $k > k_F$.

The spectral function can be written in the Lehmann representation on the real axis as:

$$A(\mathbf{k}, \omega > \mu) = \sum_{\nu} |\langle \phi_{\nu}^{N+1} | c_{\mathbf{k}\sigma}^{\dagger} | \phi_0^N \rangle|^2 \delta(\omega - E_{\nu}^{N+1} + E_0^N) \quad (12)$$

$$A(\mathbf{k}, \omega < \mu) = \sum_{\nu} |\langle \phi_{\nu}^{N-1} | c_{\mathbf{k}\sigma} | \phi_0^N \rangle|^2 \delta(\omega - E_0^N + E_{\nu}^{N-1})$$

$A(\mathbf{k}, \omega)$ has structure at the energies of the excitation of the system with one added particle ($\omega > \mu$) or one removed particle ($\omega < \mu$). The result of Fig. 3 can be understood from the low energy excitation of the system when $g = 0$. These are listed in Table I and the corresponding excitation energies are shown in Fig. 4. For $g = 0$ all the weight is in the main band labeled $\xi_{\mathbf{k}}$ because the matrix elements in Eq. (12) vanish when one boson is present. The effect of a finite g is to give some spectral weight to the “shadow” band at $\xi_{\mathbf{k}-\mathbf{Q}} \pm \omega_0$ and to introduce some level repulsion when the bands cross. The important point is that the shadow band never touches the Fermi level but it is separated from it by the energy to create the bosonic excitation. We associate the main band with the quasiparticle band and the shadow band with the incoherent spectral weight. Clearly close enough to the Fermi level only the quasiparticle band exist.

Addition $\omega > 0$		
State	$E_{\nu}^{N+1} - E_0^N$	Momentum
$c_{\mathbf{k}\sigma}^{\dagger} \phi_0^N \rangle$	$\xi_{\mathbf{k}}$	\mathbf{k}
$c_{\mathbf{k}-\mathbf{Q}\sigma}^{\dagger} b_{\mathbf{Q}}^{\dagger} \phi_0^N \rangle$	$\xi_{\mathbf{k}-\mathbf{Q}} + \omega_0$	\mathbf{k}
Removal $\omega < 0$		
State	$E_0^N - E_{\nu}^{N-1}$	Momentum
$c_{-\mathbf{k}\sigma} \phi_0^N \rangle$	$\xi_{-\mathbf{k}}$	\mathbf{k}
$c_{-\mathbf{k}+\mathbf{Q}\sigma} b_{-\mathbf{Q}}^{\dagger} \phi_0^N \rangle$	$\xi_{-\mathbf{k}+\mathbf{Q}} - \omega_0$	\mathbf{k}

TABLE I: Low energy excitations in the $g = 0$ limit. The central column shows the excitation energy. Notice that $\xi_{-\mathbf{k}} = \xi_{\mathbf{k}}$.

Notice that the shadow bands are quite similar to the case of a symmetry-broken state (but for a shift in energy of order $\omega_0 = 0.3$, which is small on the scale of the hopping $t = 1$).

Because the QP states at the Fermi level are negligibly affected by the scattering with the dynamical ordering mode, the FS (here represented by points) is preserved and no shadow branches appear at low energy. Therefore already this simple weak-coupling case shows that an ordered state would be inferred from the presence of shadow bands at high energies, while the low-energy QP are characteristic of a uniform state.

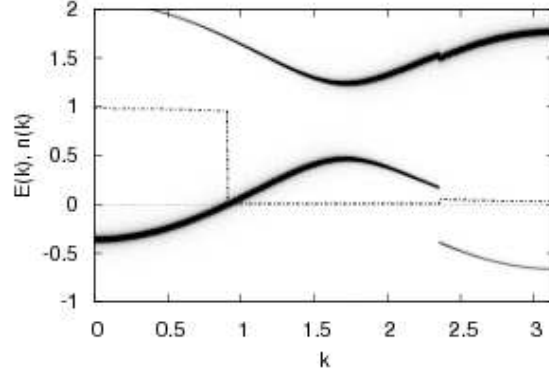


FIG. 3: Two-pole band structure in one dimension for $g^2/\omega_0 = 0.5$, $\omega_0 = 0.3$ and electron density $n = 0.57$. The width of the curve is proportional to the weight of the state. The dashed curve is the momentum distribution curve.

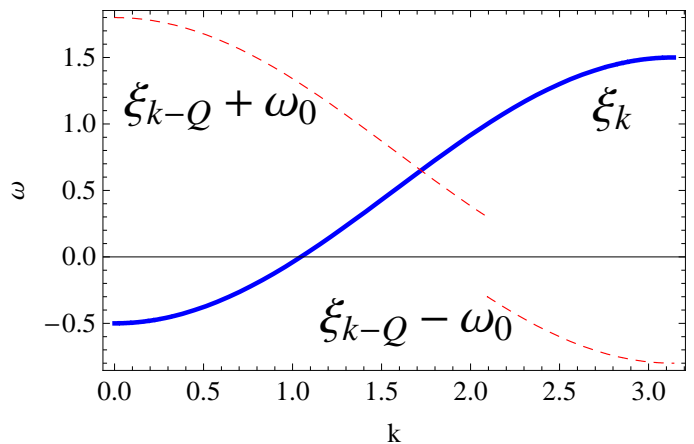


FIG. 4: Schematic electronic structure for $g = 0$.

In Fig. 3 we also report the momentum distribution $n_{\mathbf{k}}$. From this quantity one can see that some weight is indeed present at high energy via the shadow band appearing at momenta above $k^* \approx 2.3$. This is a signature of some ordering in the system. However, since the CO/SO is dynamical the dispersion discontinuously jumps from above to below the Fermi level without producing an additional branch to the FS and with no violation of the Luttinger theorem. In this last respect we explicitly checked that the Green function at zero frequency is positive for $k < k_F$, it changes sign through a pole at k_F and stays negative all the way up to π . The Fermi momentum k_F is the same that one would have in a non-interacting tight-binding system with the same number of particles $k_F = n\pi/2$ with $n = 0.57$ in this case.

The above picture remains valid if additional poles are considered in the Green function provided the QP-CO/SO-mode coupling is in a weak-to-moderate regime.

Fig. 5 reports the case of three poles for the same parameters of Fig. 3. The increased allowed number of poles

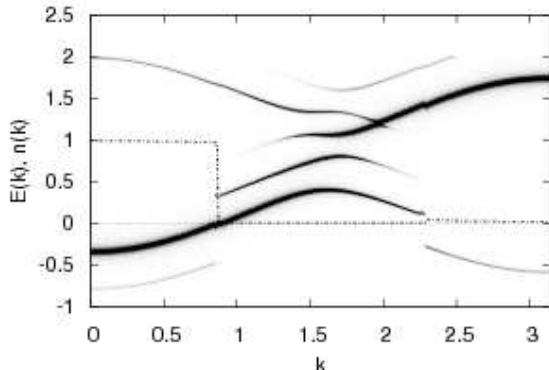


FIG. 5: Six-pole band structure in one dimension for $g^2/\omega_0 = 0.5$ and $\omega_0 = 0.2$. The electron density is $n = 0.55$. The width of the curve is proportional to the weight of the state.

better represents the shift of spectral weight at high energies induced by multiple shadow bands. Nevertheless, the finite frequency of the mode protects the low-energy QPs from being scattered and leaves the low-energy spectrum unaffected: The FS is still formed by just two points despite the appearance of several shadow bands at high energy typical of a CO/SO state. The effect of the self consistency is to “blur” the shadow bands but still the incoherent spectral weight retains a strong momentum dependence.

Upon increasing the QP-CO/SO mode coupling g one eventually enters a regime where our non-crossing perturbative scheme neglecting vertex corrections breaks down and the Luttinger theorem is violated. This situation is reported in Fig. 6, where a second branch of the FS appears due to the strong bending down of the band at momenta $k \approx k^*$. In this case the Green function at zero frequency $G(\omega = 0)$ changes sign twice (and diverges) at the two Fermi momenta k_{F1} and k_{F2} while it changes sign passing through zero at $k = k^*$, where the jump in the dispersion below μ signals a divergence of the self-energy (11). One can check explicitly that the volume corresponding to a positive $G(\omega = 0)$ is larger than the one given by occupied states in the non-interacting system thus Luttinger theorem is not satisfied. We believe this is an artifact due to the lack of vertex corrections which become important as the coupling is increased.

The apparent success of this simple theory on illustrating the spectral function of a system with fluctuating order is encouraging. However a different problem arise if one considers the half-filling case. Without long range order we would expect a metallic state if we where able to solve the model exactly. On the contrary commensurate scattering in the perturbative solution produces the unphysical result of a gapped FS in contrast with the fact

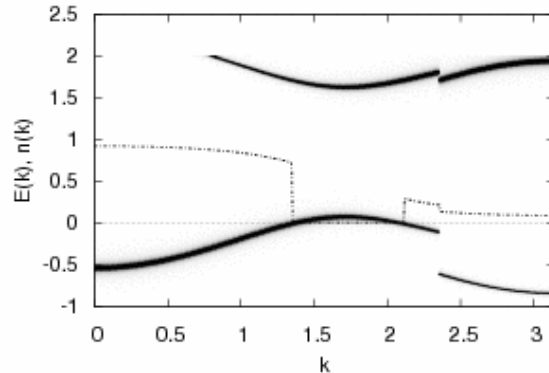


FIG. 6: Two-pole band structure in one dimension for $g^2/\omega_0 = 2$. and $\omega_0 = 0.3$. The electron density is $n = 0.83$. The width of the curve is proportional to the weight of the state. The dashed curve is the momentum distribution curve.

that no true broken symmetry is present in the system. On the other hand it is not surprising that our perturbative approach fails when our singular interaction $\chi(\mathbf{q}, \omega)$ connects two degenerate states at the FS as it occurs in this case. We believe this failure is due to the lack of vertex corrections which we expect should suppress the scattering at the Fermi level. We have tested this idea phenomenologically by assuming that the QPs at the Fermi level are protected against this singular scattering by a momentum dependence of the coupling of the form

$$\tilde{g}(\tilde{\varepsilon}_{\mathbf{k}}, \tilde{\varepsilon}_{\mathbf{k}+\mathbf{q}}) = g \tanh\left(\frac{\tilde{\varepsilon}_{\mathbf{k}}}{\omega_0}\right) \tanh\left(\frac{\tilde{\varepsilon}_{\mathbf{k}+\mathbf{q}}}{\omega_0}\right) \quad (13)$$

One technical remark is in order here. Perturbatively one could introduce on the r.h.s. of Eq. (13) the bare QP dispersion $\varepsilon_{\mathbf{k}}$. However, at moderate-strong couplings the QP dispersions are substantially modified by the coupling with the modes to dressed QP dispersions $\tilde{\varepsilon}_{\mathbf{k}}$. To suppress the scattering of the *dressed* QPs near the true FS, one must insert in (13) the renormalized dispersions $\tilde{\varepsilon}_{\mathbf{k}}$. This need of a self-consistency scheme considerably complicates the calculations and lead us to consider only simple symmetry breakings (cell doublings).

Although the form (13) is adopted on a purely phenomenological basis, we like to remind that several microscopic calculations^{20,21} show that in strongly correlated systems the coupling between QPs and phonons is severely suppressed at low energies. This suppression is mostly effective when the exchanged momenta $v_F \mathbf{q}$ are larger than the typical exchanged energy ω_0 . This is the case here, where the exchanged momenta are peaked at sizable \mathbf{Q} 's.

Figs. 7(a) and (b) illustrate the effect of this vertex correction in the half-filled case $n = 1$, where it plays a crucial role to restore the metallicity of the system.

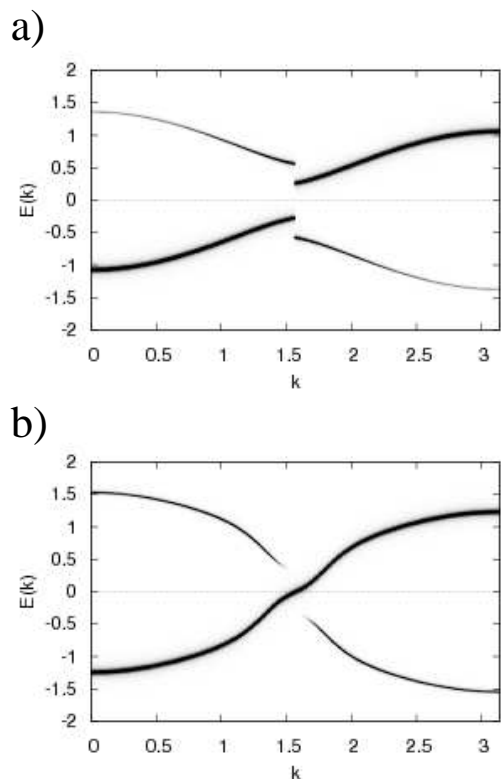


FIG. 7: Two-pole band structure in one dimension for $g^2/\omega_0 = 0.5$ and $\omega_0 = 0.3$ at half-filling $n = 1$. In (a) the bare vertex g is used, while in (b) the phenomenological vertex \tilde{g} of Eq. (13) is used.

For the previously considered cases of generic filling we find that the vertex corrections play a minor role and the results obtained with \tilde{g} differ little at moderate coupling from those reported above. However, for strong coupling the phenomenological form of the vertex Eq. (13) again prevents the system to violate Luttinger theorem as e.g. in case of the result shown in Fig. 6.

Finite range fluctuations

Since in realistic systems the dynamical fluctuations have a finite coherence length and a finite lifetime, we also investigated the case of a one-dimensional QP band exposed to fluctuations having finite Γ and γ in $F_{\omega_0, \Gamma}$ and in Eq. (5). Obviously the finite extension in space and time of the fluctuations produces broadening in the spectra. As it is natural, one finds that the broadening in the momentum direction is ruled by γ , while Γ rules the broadening along the energy axis. As it clearly appears in Fig. 8, the broadening of the spectra does not spoil the essential feature of the coupling with a dynamical mode (cf. Fig. 3 for $\gamma = \Gamma = 0$ but same parameters otherwise): The shadow bands persist as high-energy signatures of a (local) order, while the FS stays unchanged

and Luttinger theorem is obeyed provided the mode is sufficiently narrow in energy ($\gamma < \omega_0$) so that one can neglect the “leakage” of weight down to the Fermi level.

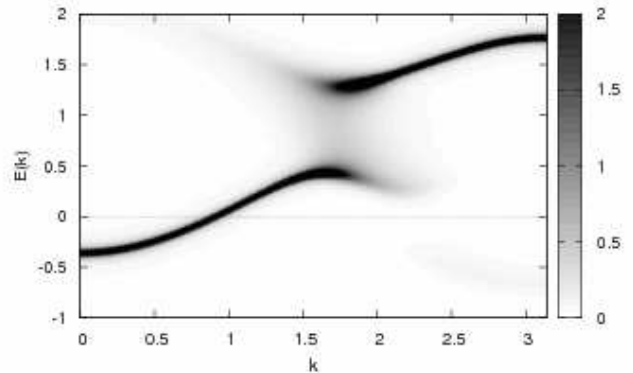


FIG. 8: Two-pole band structure in one dimension for $g^2/\omega_0 = 0.5$ and $\omega_0 = 0.3$ at generic filling $n = 0.57$. Here a finite inverse coherence length $\gamma = 0.02$ and time $\Gamma = 0.1$ are used.

Pairing effects

We further explore our one-dimensional model to investigate the effects of a particle-particle pairing. To this purpose we introduce in our bare QP band structure a finite gap Δ , which, as it is usual for this type of pairing, is tight to the FS. Accordingly the Bogoliubov particle-hole mixing occurs near the FS and the QP band opens a gap centered at the Fermi level. The branch below the Fermi level bends down giving rise to a maximum occurring at a momentum coinciding with the Fermi momentum of the unpaired QPs. Fig. 9 displays this effect for our typical parameter set at a generic filling. In particular one can see that the particle-particle pairing only modifies the low-energy states over scales of order Δ , while leaving unchanged the high-energy states, which still display the clear effect of the dynamical ordering.

B. Numerical analysis in two dimensions

Once the main effects of the dynamical mode exchange have been presented in one dimension, we illustrate the two-dimensional case. For the bare electron dispersion we use:

$$\varepsilon_{\mathbf{k}} = -2t(\cos(k_x) + \cos(k_y)) + 4t' \cos(k_x) \cos(k_y)$$

For concreteness the parameters have been chosen to reproduce the FS of LSCO, taking $t = 342$ meV, $t'/t = -0.2$, and $\mu = -0.1t$. For the mode frequency and coupling, we choose $\omega_0 = 50$ meV and $g^2 = 1.5\omega_0$, while we

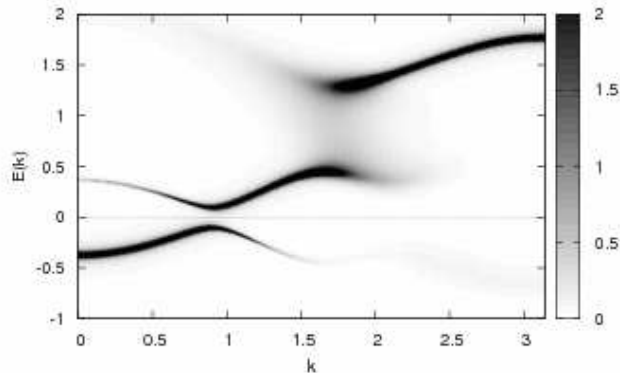


FIG. 9: Two-pole band structure in one dimension for $g^2/\omega_0 = 0.5$ and $\omega_0 = 0.3$ at generic filling $n = 0.4$. Here a finite inverse coherence length $\gamma = 0.02$ and time $\Gamma = 0.1$ are used as well as a finite pairing gap $\Delta = 0.1$.

consider only coherent fluctuations with vanishing broadenings ($\Gamma = \gamma = 0$). To avoid too many band foldings, which could complicate the analysis, we choose a order given by a simple cell doubling in the x direction. This gives rise to $\mathbf{Q} = (\pm\pi, 0)$. Of course this does not correspond to the charge/spin modulation observed in LSCO cuprates, but it better fits our simplicity and illustrative purposes (on the other hand it corresponds to the spin ordering in FeAs stoichiometric compounds^{22,23}).

Figs. 10 (a) and (b) report the two-dimensional FS obtained by integrating the spectral density in Eq. (1) over a small ($W_l = 10$ meV) and a large ($W_h = 100$ meV) energy range respectively. Only two poles have been considered in the recursive GF and the QP-mode coupling is dressed via the 'self-consistent' vertex corrections [i.e. corrected by the interaction itself, see the remark after Eq. (13)]. These corrections are required here because at the typical fillings we consider, the two-dimensional FS has branches connected by the critical wavevectors (the so-called "hot spots" in the framework of superconducting cuprates). The states connected by \mathbf{Q} would display a gap opening similar to the (spurious) one obtained in one dimension at $n = 1$. For this reason we decided to phenomenologically suppress this exceedingly strong effect which we attribute to the simple perturbative treatment of the singular interactions in the model.

In the case of integration over the low-energy states only, one obtains a FS closely resembling the one of unperturbed free QPs'. On the contrary, upon integrating over a broad energy range, the "FS" appears folded and closely tracks the one expected for a system with a static long-ranged broken symmetry. Therefore, also in two dimensions we see that coupling the QPs with *dynamical* modes preserves the QPs from a strong rearrangement of all the states (including those near the FS). Notice that the vertex corrections are relevant in this regard only

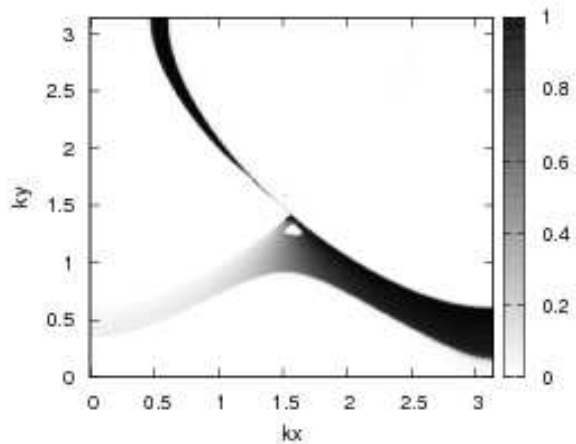
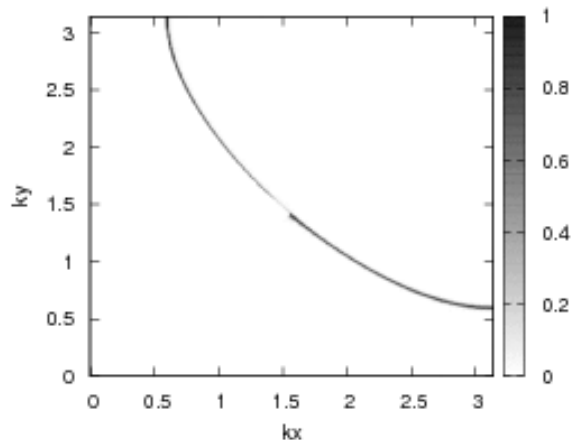


FIG. 10: Two dimensional FS obtained from the momentum distribution function $n_{\mathbf{k}}$ in Eq. (1). The spectral function has been integrated over: (a) a low-energy range $W_l = 10$ meV; (b) a high-energy range $W_h = 100$ meV.

around the hot spots, but do not prevent the generic formation of shadow bands or related features appearing in $n_{\mathbf{k}}$.

IV. DISCUSSION AND CONCLUSIONS

The results of the previous sections clearly indicate that *dynamical* CO/SO fluctuations, at least in a not too strong coupling regime, do not produce substantial effects on QPs around the FS. Therefore the absence of low-energy signatures of CO/SO is compatible with a dynamical type of order. Our computations are restricted to weak coupling therefore quasiparticle weights are close

to one and the incoherent weights are small. To have the reverse ratios of weight we need to go to strong coupling, which is unfortunately not feasible. Therefore we can only speculate on how the spectral function will look like.

We expect that as the coupling is increased some features of our computations will persist. For example the fact that the momentum dependent incoherent part of the spectral function is separated by a bosonic excitation from the Fermi level is expected to be quite robust in strong coupling. Indeed one can construct approximated excitations as in Table I but with heavily dressed quasiparticles rather than with particles which suggest that a similar physics will be at play. More complicated excitations may give spectral weight closer to the Fermi level but for those the momentum dependence will be completely washed out providing a structureless background.

The fact that the incoherent part should resemble the electronic structure of the ordered state follows from continuity arguments. For example, as one crosses a transition where the spin gets disordered at low energies one does not expect dramatic changes in the overall distributions of weight in the spectral functions. Those will be determined to a large extent by the short range correlations which may change very little across the order disorder transition. In this sense a faint quasiparticle peak emerging at low energies, which is certainly a dramatic perturbation from the point of view of the Fermi liquid properties becomes a small perturbation from the point of view of the spectral weight distribution. Thus we expect this resemblance to persist in the strong coupling limit.

The scenario we propose is of obvious pertinence in cuprates, where standard ARPES experiments usually report a Fermi-liquid Fermi surface while other experiments display the signatures of dynamic order like the famous hourglass dispersion relation observed in cuprates²⁴ even when CO/SO is not detected.^{25,26} This hourglass dispersion has been explained computing the fluctuations on top of an ordered ground state.⁹ Our analysis might help to reconcile this contradictory experimental situation.

One difficulty in interpreting data in the cuprates is the presence of disorder. It is possible that the system has an ordered ground state but, due to quenched disorder or a complex energy landscape²⁷, it never becomes ordered. As for a structural glass, the system has long range in time positional order but a structural factor characteristic of a disordered state. In this case scattering probes will fail to detect order even though the charge is not fluctuating and is inhomogeneous. Local probes, however, should be able to detect the ordering but those are more scarce and more difficult to interpret. Both static disorder and our picture will predict similar results at high energies but will strongly differ at low energies were only within our picture one recovers a uniform Fermi liquid. It is not clear at the moment which effect prevails in different experiments.

There are cases in which CO has been detected^{28,29,30}

and still the stripe Fermi surface computed in LDA⁸ and measured from the $n_{\mathbf{k}}$ does not show up close to the Fermi level. For example no visible shadow FS's appears in Ref. 31, where the FS of a CO LSCO sample only displayed Fermi arcs due to a particle-particle pseudogap. It is possible that in this case the system charge orders because the commensuration with the underlying lattice provides a pinning potential, which helps to stabilize the charge but the spin is still quantum disordered. One should keep in mind that spin order breaks a continuous symmetry whereas commensurate CO, as usually observed in cuprates, only breaks a discrete symmetry. Therefore the former is much more fragile than the latter. Thus we propose a state in which the charge is ordered but for the spin our dynamical picture applies. One can still wonder why one does not see shadows due to the CO. One should keep in mind that the CO is a minor perturbation to the electrons compared to SO. In a SO state the effective potential seen by the electrons oscillates on a scale of U . In order to check the effect of CO alone without SO we have computed the FS in the presence of a charge modulation similar to the one observed. The result is a large Fermi liquid like FS with small features due to the CO which will be difficult to detect in practice.³² It is only at moderate energies, above ω_0 for the magnetic excitations, that the mixed CO-SO fluctuations produce shadow features in the spectra and give rise to "crossed FS's" like those observed in LSCO in Refs. 6,7.

A momentum dependence of the so-called "hump" features at relatively high energies (of order 0.1 eV) has also been detected in $\text{Bi}_2\text{Sr}_2\text{CaCu}_2\text{O}_{8+\delta}$ ³³. This was attributed to quasiparticles scattering with the (π, π) spin resonance created below T_c . However, the persistence of dispersion above T_c in the pseudogap regime indicates that this dispersion could (at least partially) arise from a "hidden" SO like the one investigated here. An analysis of $n_{\mathbf{k}}$ similar to the one carried out for LSCO in Refs. 6,7 could also help in discerning whether this is just a remnant effect of the proximity to the insulating antiferromagnet or due to fluctuating stripes.

In conclusion, in the light of the analysis carried out in this paper, we propose that cuprates are affected by finite-energy spin fluctuations related to the tendency to order. Whether this CO is actually realized in a static way is rather immaterial from the point of view of low-energy ARPES spectra due to the weakness of the charge modulations. Only when the energy is above the spin and charge fluctuating scale the electronic spectrum is sizably affected. At these energies, however, the detection of CO-SO-related pseudogaps (not tied to the FS) is quite hard due to the largely incoherent character of the spectral lines. Only passing through n_k this dynamical tendency to CO becomes visible.

We acknowledge interesting discussions with C. Castellani, C. Di Castro. M. G. acknowledges financial support from MIUR Cofin 2005 n. 2005022492 and M.G and G. S. from the Vigoni foundation.

APPENDIX A: ITERATIVE SOLUTION OF THE MODEL

In this Appendix we give a detailed description of the iterative solution of the two coupled equations (9,10). Inserting the lowest-order self-energy $\Sigma^{(1)}(k, i\omega)$ (Eq. (11)) into Eq. (10) leads to a $G^{(1)}(k, i\omega)$ which displays two poles and which can be used to compute $\Sigma^{(2)}(k+Q, i\omega)$ (and thus $G^{(2)}(k+Q, i\omega)$) and so on. This procedure therefore generates the series

$$\begin{aligned} G^{(1)}(k, i\omega) &\rightarrow G^{(2)}(k+Q, i\omega) \rightarrow G^{(3)}(k, i\omega) \\ &\rightarrow G^{(4)}(k+Q, i\omega) \rightarrow G^{(5)}(k, i\omega) \cdots \rightarrow G^{(n-1)}(k+Q, i\omega) \end{aligned}$$

where $G^{(n-1)}(k+Q, i\omega)$ has a n -pole structure that can be represented as

$$G^{(n-1)}(k+Q, i\omega) = \sum_{s=1}^n \frac{[\alpha_s^{(n)}(k)]^2}{i\omega - E_s^{(n)}(k)}. \quad (\text{A1})$$

Consequently the n -th order for the self-energy is given by

$$\Sigma^{(n)}(k, i\omega) = g^2 \sum_{s=1}^n \frac{[\alpha_s^{(n)}(k)]^2}{i\omega \pm \omega_0 - E_s^{(n)}(k)} \quad (\text{A2})$$

and the sign of ω_0 in the denominator depends on whether $f(E_s^{(n)}(k)) = 0, 1$ (cf. Eq. (11)).

Examining the equation for the n -order GF $(i\omega - \varepsilon_k - \Sigma^{(n+1)})G^{(n+1)} = 1$ it turns out that the solution can be conveniently obtained by solving the matrix equation:

$$[i\omega \underline{\mathbb{1}} - \underline{\underline{M}}] \underline{\underline{K}} = \underline{\underline{\mathbb{1}}} \quad (\text{A3})$$

with

$$\underline{\underline{M}} = \begin{pmatrix} \varepsilon_k & g\alpha_1^{(n)}(k) & g\alpha_2^{(n)}(k) & \cdots & g\alpha_n^{(n)}(k) \\ g\alpha_1^{(n)}(k) & E_1^{(n)}(k) \mp \omega_0 & 0 & \cdots & 0 \\ g\alpha_2^{(n)}(k) & 0 & E_2^{(n)}(k) \mp \omega_0 & \cdots & 0 \\ \vdots & \vdots & \vdots & \vdots & \vdots \\ \cdots & \cdots & \cdots & \cdots & \cdots \\ \vdots & \vdots & \vdots & \vdots & \vdots \\ g\alpha_n^{(n)}(k) & 0 & 0 & \cdots & E_n^{(n)}(k) \mp \omega_0 \end{pmatrix}. \quad (\text{A4})$$

and we can identify the (n) -order GF as the (11) -element of the matrix $\underline{\underline{K}}$. Denoting by $\underline{\underline{T}}$ the transformation which diagonalizes $\underline{\underline{M}}$, thereby yielding $(n+1)$ eigenvalues $E_s^{(n+1)}(k)$, the (n) -order GF is thus obtained as

$$G^{(n)}(k, i\omega) = \sum_{s=1}^{n+1} \frac{[T_{1s}]^2}{i\omega - E_s^{(n+1)}(k)} \quad (\text{A5})$$

which also yields the new weights $\alpha_s^{(n+1)}(k) \equiv T_{1s}$.

This scheme allows for a systematic evaluation of the GF up to some given order (n) . In the first step, the ma-

trix $\underline{\underline{M}}$ is of order 2×2 with $\alpha_1^{(1)}(k) = 1$ (cf. Eq. (9)) and $E_n^{(1)}(k) = \varepsilon_{k+Q}$. Diagonalization yields the weights and energies of $G^{(1)}(k, i\omega)$ which can be used to construct the matrix for $G^{(2)}(k+Q, i\omega)$ (where the (11) -element of $\underline{\underline{M}}$ in Eq. (A4) is ε_{k+Q}) and so on. This procedure creates spectral functions with more and more poles, however, in case of a not too strong coupling, it will converge in the sense that the weight of newly created poles becomes smaller and smaller so that the series can be cut at the desired accuracy.

¹ A. Georges, G. Kotliar, W. Krauth, and M. J. Rozenberg, Rev. Mod. Phys. **68**, 13 (1996).

² M. Imada, A. Fujimori, and Y. Tokura, Rev. Mod. Phys. **70**, 1039 (1998).

³ C. Castellani, C. Di Castro, and M. Grilli, Journal of Physics and Chemistry of Solids **59**, 1694 (1998).

⁴ S. A. Kivelson, E. Fradkin, and V. J. Emery, Nature (London) **393**, 550 (1998).

⁵ J. Zaanen, O. Y. Osman, H. Eskes, and W. van Saarloos, J. Low Temp. Phys. **105**, 569 (1996).

⁶ X. J. Zhou, P. Bogdanov, S. A. Kellar, T. Noda, H. Eisaki, S. Uchida, Z. Hussain, and Z. X. Shen, Science **286**, 268 (1999).

⁷ X. J. Zhou, T. Yoshida, S. A. Kellar, P. V. Bogdanov, E. D. Lu, A. Lanzara, M. Nakamura, T. Noda, T. Kakeshita, H. Eisaki, S. Uchida, A. Fujimori, Z. Hussain, and Z. X. Shen,

- Phys. Rev. Lett. **86**, 5578 (2001).
- ⁸ V. I. Anisimov, M. A. Korotin, A. S. Mylnikova, A. V. Kozhevnikov, D. Korotin, and J. Lorenzana, Phys. Rev. B **70**, 172501 (2004).
 - ⁹ G. Seibold and J. Lorenzana, Phys. Rev. Lett. **94**, 107006 (2005).
 - ¹⁰ J. Lorenzana and G. Seibold, Phys. Rev. Lett. **90**, 066404 (2003).
 - ¹¹ A. P. Kampf and J. R. Schrieffer, Phys. Rev. B **42**, 7967 (1990).
 - ¹² G. Seibold and M. Grilli, Phys. Rev. B **63**, 224505 (2001).
 - ¹³ G. H. Gweon, T. Sasagawa, S. Y. Zhou, J. Graf, H. Takagi, D. H. Lee, and A. Lanzara, Nature **430**, 187 (2004).
 - ¹⁴ H. Iwasawa, Y. Aiura, T. Saitoh, H. Eisaki, H. Bando, A. Ino, M. Arita, K. Shimada, H. Namatame, M. Taniguchi, T. Masui, S. Tajima, M. Ishikado, K. Fujita, S. Uchida, J.F. Douglas, Z. Sun, D.S. Dessau, Physica C **463**, 52 (2007).
 - ¹⁵ G. Seibold and M. Grilli, Phys. Rev. B **72**, 104519 (2005).
 - ¹⁶ S. Engelsberg and J. R. Schrieffer, Phys. Rev. **131**, 993 (1963).
 - ¹⁷ G. Seibold, F. Becca, F. Bucci, C. Castellani, C. Di Castro, and M. Grilli, Europ. Phys. J. B **13**, 87 (2000).
 - ¹⁸ P. A. Lee, T. M. Rice, and P. W. Anderson, Phys. Rev. Lett. **31**, 462 (1973).
 - ¹⁹ A. Posazhennikova and P. Coleman, Phys. Rev. B **67**, 165109 (2003).
 - ²⁰ M. Grilli and C. Castellani, Phys. Rev. B **50**, 16880 (1994).
 - ²¹ G. Sangiovanni, M. Capone, C. Castellani, and M. Grilli, Phys. Rev. Lett. **94**, 026401 (2005).
 - ²² J. Dong, H. J. Zhang, G. Xu, Z. Li, G. Li, W. Z. Hu, D. Wu, G. F. Chen, X. Dai, J. L. Luo, Z. Fang, and N. L. Wang, Competing Orders and Spin-Density-Wave Instability in $\text{La}(\text{O}_{1-x}\text{F}_x)\text{FeAs}$, arXiv:0803.3426, 2008.
 - ²³ Clarina de la Cruz, Q. Huang, J. W. Lynn, J. Li, R. W. Li, J. L. Zarestky, H. A. Mook, G. F. Chen, J. L. Luo, N. L. Wang, and P. Dai, Magnetic order versus superconductivity in the Iron-based layered $\text{La}(\text{O}_{1-x}\text{F}_x)\text{FeAs}$ systems, arXiv:0804.0795, 2008.
 - ²⁴ J. M. Tranquada, H. Woo, T. G. Perring, H. Goka, G. D. Gu, G. Xu, M. Fujita, and K. Yamada, Nature (London) **429**, 534 (2004).
 - ²⁵ S. M. Hayden, H. A. Mook, P. Dai, T. G. Perring, and F. Dogan, Nature (London) **429**, 531 (2004).
 - ²⁶ N. B. Christensen, D. F. Mcmorrow, H. M. Rønnow, B. Lake, S. M. Hayden, G. Aeppli, T. G. Perring, M. Mangkorntong, M. Nohara, and H. Tagaki, Phys. Rev. Lett. **93**, 147002 (2004).
 - ²⁷ J. Schmalian and P. G. Wolynes, Phys. Rev. Lett. **85**, 836 (2000).
 - ²⁸ J. M. Tranquada, B. J. Sternlieb, J. D. Axe, Y. Nakamura, and S. Uchida, Nature (London) **375**, 561 (1995).
 - ²⁹ P. Abbamonte, A. Rusydi, S. Smadici, G. D. Gu, G. A. Sawatzky, and D. L. Feng, Nature Phys. **1**, 155 (2005).
 - ³⁰ Y. Kohsaka, C. Taylor, K. Fujita, A. Schmidt, C. Lupien, T. Hanaguri, M. Azuma, M. Takano, H. Eisaki, H. Takagi, S. Uchida, and J. C. Davis, Science **315**, 1380 (2007).
 - ³¹ T. Valla, A. V. Fedorov, J. Lee, J. C. Davis, and G. D. Gu, Science **314**, 1914 (2006).
 - ³² A. Di Ciolo, M. Grilli, J. Lorenzana, and G. Seibold, Phys. C **460-462**, 1176 (2007).
 - ³³ J. C. Campuzano, H. Ding, M. R. Norman, H. M. Fretwell, M. Randeria, A. Kaminski, J. Mesot, T. Takeuchi, T. Sato, T. Yokoya, T. Takahashi, T. Mochiku, K. Kadowaki, P. Guptasarma, D. G. Hinks, Z. Konstantinovic, Z. Z. Li, and H. Raffy, Phys. Rev. Lett. **83**, 379 (1999).